Wear and Corrosion of Wrought A6061 Aluminium Alloy in DOT3 Brake Fluid

Olawale O. Ajibola*[1], Oladeji O. Ige[2], Peter A. Olubambi[3]

[1-3] Centre of NanoEngineering and Tribocorrosion, University of Johannesburg, Johannesburg, South Africa
*Corresponding author Email: olawalea@uj.ac.za

Abstract

The twofold impact of wear and corrosion on wrought A6061 alloy in hydraulic DOT3 brake fluid environment was studied. The wear studies were performed on the samples using a developed wear-jig. Weight loss corrosion test method was used to determine the corrosion rate of the wrought A6061 alloy samples immersed in the brake fluid for a total of 1680 hours. From the results of wear tests carried out on the A6061 alloy sample with brake oil, the highest wear value of 5.24×10^{-7} mg/mm^2/cycle (approx.) was obtained from 6 N (approx) force after 130 minutes. The wrought A6061 alloy material demonstrated the highest corrosion rates nearly 3.0×10^{-2} mg/mm^2/yr within the early 168 hours of immersion in brake fluid. The result is practically lower than the corrosion rate of cast specimen in DOT3 brake oil or some other alloys immersed in other corrosive media that were previously reported in the literature. The results show that small amount of chemical corrosion is sufficient to cause and accelerate mechanical wear of the material in usage.

Keywords: Hydraulic Brake Fluid; Piston Application; Wear; Wrought A6061 Alloy

1. Introduction

Aluminum alloys and hydraulic brake fluids are used in automobile braking systems for quite an age for their engineering application advantages. Meanwhile wear, fatigue failure, corrosion and oxidation are some of the limitations associated with the industrial applications of aluminum. These failure modes are surface phenomena. They emanate at the surface and can swiftly lead to stress concentration, fracture, increased friction, and other problems caused by the formation of wear debris and corrosion products occurring on rubbing or impacting surfaces [1,2]. Hence there can be corrosion induced wear or wear aggravated corrosion [3] broadly categorized under the tribocorrosion.

Although Al alloys are famous for their high strength to weight ratio, yet they are deficient for wear, high temperature applications, and many chemically aggressive environments. Aluminium can react with acids, bases and alkalis due to its amphoteric nature. Thus they are designed and manufactured with adequate consideration for their surface protection with the view to reducing the effects of wear and corrosion on surface [4-7]. Hydraulic brake and clutch master cylinders and pistons are widely made from aluminium alloys and steels [8,9]. Both faced the problems of wear (result of abrasion, high temperature resulting from two mating parts without oil, poor materials composition, and poor lubrication formulation of brake oil content). Corrosion is another problem attributed to materials composition, aluminium alloy production method, (extrusion, forged, rolled, cast), oil formulation (chemical content, amount and types of inhibitor), high temperature corrosion (formation of oxide) and moisture. The last problem combines effects of both factors of wear and corrosion resulting in tribocorrosion [10,11]. This study evaluates wear and corrosion behaviour of wrought A6061 aluminum alloy due to the contacting surfaces of the master cylinder and piston immersed in DOT 3 fluid.

The hydraulic type is the widest and the most popular of the various designs of automobile braking systems. It is expected that ideal hydraulic fluid should not corrode or at worst should not exceed the maximum permissible weight change limit of 0.1 mg/cm^2 of surface based on the SAE J1703 specification. And this may be the possible reason for scarce research reports being obtained on the behaviours of various materials (steels and aluminum alloys) used in hydraulic fluids. The majority of brake fluids are glycol-ether based, mineral oil and silicone based fluids which must meet certain required standards defined by the Society of Automotive Engineers (SAE), Department of Transport (DOT) or other government agencies [12]. Many countries operate on naming systems different from the SAE specifications [13]. The DOT3 brake oil is based on mineral oil/ silicone fluids and has its pH ranging from 10.0 to 11.5 [14]. This makes it to be alkaline and has strong potential to attack aluminium alloy components in the brake system.

Studies have been widely reported on the subjects of wear, corrosion and tribocorrosion of different Al alloys [2-3,8-11]. Aluminium alloy wears have been accessed using tribometers, while their corrosions have been studied in diverse active and aggressive media (acid, base and alkali). A few reports are available on either wear or corrosion of cast A6061 alloy [8,15] but not on the as-received wrought A6061 aluminum alloy in less aggressive organic media such brake oil environments (pH range 10.0 to 11.5) or related hydraulic fluids for automobile and hydraulic pumps applications. The reason for this work is that it is part of a research project of which the following publications are already in public domain [8, 16-21]. The results showed certain degrees of aggressiveness of the brake fluid to cast AA6061 alloy which revealed some weakness in the production of quality brake fluid likely resulting from the adulteration. Other reports centre on

EN plating on cast Al alloy assessing their performance with view to providing remedies to wear and corrosion problems of Al alloys in brake oil [22,23].

The twofold impact of abrasion and corrosion on wrought A6061 alloy in hydraulic brake fluid environment has not been reported. The present results revealed practically lower wear and corrosion rates of the specimen in brake oil than the cast Al alloys immersed in similar media that were previously reported in the literature. It shows that small amount of corrosion is sufficient to cause and accelerate mechanical wear of the material in usage. Thus discouraging the production of the master brake piston by sand casting method especially form scrap sources which are characterized by macro and micro pores.

And to ensure the reproducibility of the present work, experimentation was done using standard aluminum alloy rather than a scrap alloy previously reported [16-18]. Hence, the present research investigates wear due to abrasion and corrosion of wrought A6061 aluminum alloy in hydraulic DOT3 brake fluid with the view to understanding and improving on its wear and corrosion resistances. The laboratory experimentation was simulated and performed under relatively closed conditions to the field application using a developed wear test jig [18].

2. Methodology

2.1 Materials

The starting material for the study is wrought aluminium alloy (A6061), as-received in the form of cylindrical billet with a chemical composition (using atomic absorption spectrometer) as shown in Table 1. The hydraulic brake oil (DOT 3) properties have been described [17] elsewhere. The X-ray diffraction was done to examine phases of the A6061 alloy material using X-Ray Mini-Diffractometer (MD-10 model) and the results are shown in Table 2.

Table1: Chemical Composition of A6061 Alloy Sample

Element	Al	Si	Mg	Fe	Ti
Composition [%]	98.87	0.38	0.40	0.23	0.001
Element	Mn	Cu	Zn	Cr	Ti
Composition [%]	0.001	0.01	0.001	0.001	0.001

2.2 Preparation of test samples

For the wear experiment, the A6061 alloy specimen was cut and was shaped to the 100 mm long by 12 mm diameter size featured specimen (Fig. 1a) using the lathe and the universal milling machine. In case of the corrosion test, samples were cut to 25 mm diameter and 15 mm thickness using hack saw (Fig. 1c). The specimens were polished using 400~1200 µm grit papers/cloth to get uniform and smooth surface.
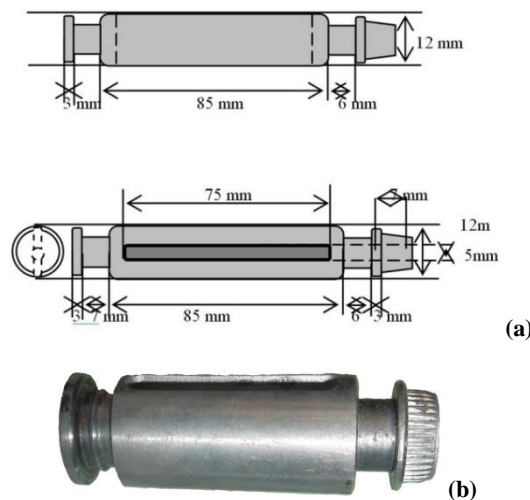

(a)

(b)

(c)

Fig. 1: (a) Sketch diagrams, photographs of (b) piston specimens and (c) coupon for corrosion tests

Table 2: XRD Analysis of Al alloy Sample

Diffr. angle (2θ)	Peak	Phases	Structures
27.6803	0.25	$MgO.Al_2O_3$	Tetragonal
64.7793	0.35	AlCu	Monoclinic
37.8674	1.80	$CuAl_2$	Tetragonal
46.1875	0.95	AlCu	Monoclinic
68.2625	0.20	$Al_2Si_4O_{10}$	Triclinic
23.0124	0.20	$Al_2Si_4O_{10}$	Triclinic
32.2546	0.15	$Al_2Si_4O_{10}$	Triclinic
51.2504	0.35	$Al_2Si_4O_{10}$	Triclinic
59.7511	0.20	$CuAl_2$	Cubic
46.7107	0.10	SiO_2	Monoclinic
56.0038	0.15	SiO_2	Monoclinic

2.3 Wear of samples with and without hydraulic fluid

The wear tests (dry and wet) were performed to determine the wear rate of the A6061 alloy material with and without fluid. The wear test jig machine was designed and operated according to the SAE-J1154-1983; considering ASTM G-119-04 and it has been described in the previous reports [8]. The alternative system described in SAE J1703 is a stroking test procedure used to assess the lubricating quality of DOT3 brake oil on the wear of Al alloy piston. The master cylinder Assembly (with master cylinder of 28 mm approx diameter) and the pressure actuating mechanism with push rod without side thrust, the force applied by the actuating mechanism is adjustable, capable of supplying sufficient stroke (500-3100 min^{-1}) and thrust to the master cylinder to get pressure of at least 70 kg/cm^2 in the simulated braking system. The specimen (Fig. 1a) was inserted into the cylinder of the wear test jig machine (Fig. 2) after measuring the initial weight of the specimen. The machine is electrically powered having stroke of 26 mm, and causing mechanical jigging action on the wrought A6061 alloy specimen. The repeated to and fro movements cause the specimen surface to experience wear (Fig. 2) against the cylinder wall, with and without fluid. The wear time was varied for 10 to 220 minutes to give sufficiently long contact period. The final weight of the specimen after each wear time was determined by using a digital weighing machine measured to 0.0001 g. Multiple wear tests were performed on test specimens and the average value was taken as a measure of the wear parameters (weight loss, volume loss) to determine the wear rate and wear resistance of the specimen.
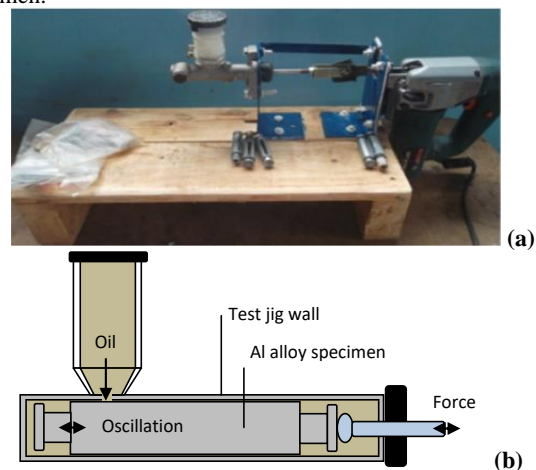

(a)

(b)

Fig. 2: Showing (a) pictorial and (b) cross section of wear test jig [8, 17, 18].

The loss to wear (W_L) was determined by measuring the weight difference (ΔW) between the original weight (W_i) and the final weight (W_f) of the specimen after wear exposure in equation (1),

$$W_L = \Delta W = W_f - W_i \tag{1}$$

The Wear volume (V_w) of aluminium alloy sample during the experiment was determined from the material density (ρ_m) in equation (2),

$$V_w = m/\rho_m = \Delta W /\rho_m \tag{2}$$

This is also used in determining the Wear rate W_r (3) and Wear resistance R_w

$$W_r = \Delta W/A_s t \tag{3}$$

where m is the loss to wear W_L or ΔW (g), V_w is the wear volume loss (cm^3 or mm^3), ρ_m is the material density (gcm^{-3}or gmm^{-3}), A_s is the surface area (mm^2) and t is the wear exposure time (minutes) Using Equation 2, the wear volume V_w with respect to the change in cross sectional area is given as in (4),

$$\Delta A_c \; x \; L = \rho_m /\Delta W \tag{4}$$

where ΔA_c is the change in cross sectional area, L is the length of contact surface of specimen.
The volume of wear that can occur is described by Archard's equation in (5),

$$V_w = A_c \, d \tag{5}$$

where V_w is the volume of wear volume, A_c is the cross-sectional area, and d is the distance slid [5] which in the present case d is the same as L
Wear resistance R_w, is simply defined as the reciprocal of wear volume V_w (in cm^{-3} or mm^{-3}) as Equation 6.

$$R_{w'} = 1/V_w \tag{6}$$

The effect of wear on the physical properties such as the appearance, colour and roughness of the wrought A6061 alloy surface was examined under high resolution microscopic camera and SEM.

2.4 Determination of corrosion rate

The weight loss method by full immersion was employed to assess the corrosion damages and corrosion rates of the wrought A6061 alloy samples in the DOT3 fluid medium. After the expected and stipulated immersion time, the specimens were removed, rinsed in water and dried with cotton wool to remove water and other impurities. The weight loss to corrosion ΔW_c (g) was determined from the difference between the initial weight (M_i) and final weight (M_f) of the sample before and after immersion respectively. About 3 to 4 weight loss readings were measured using a digital weight meter (0.0001g) and the average value was used to calculate the corrosion rate for each day. The immersed specimens were examined daily for 10 weeks (1680 hrs). Corrosion experiments were prepared, performed, analysed and reported considering the ASTM G 161-00, G 1-03, G 4-01, G 16-95(2004), G31-72(2004), G 40-02; and the NACE standard TM0169-2000. The corrosion rate was calculated according to ASTM G-119-04 [24].

2.5 Surface characterization

The corroded and worn surfaces of the test specimen were examined using the field emission scanning electron microscope (Jeol JSM-7600F SEM) and VEGA3 TESCAN models with the EDX/EDS facilities and Zeiss MTB 2011 model metallurgical optical microscope, The microstructures, wear surface appearance, colour and roughness of specimen surfaces were also examined under high resolution microscopes. The chemical characterisation of corrosion product was assessed by EDX/EDS facilities. The results are reported as micrographs, SEM images, EDX spectra line and data.

2.6 Hardness test of samples

A five point micro-hardness tests was carried out over an area of each of the specimen surface to determine the hardness using the InnovaTest (Falcon 500 model) micro-hardness tester. The standard load of 500g was applied for a 10 sec dwell time and the average HV/0.5 value was determined and accompanied by the measurement of the diagonal of indentation d_1 and d_2. The result data and microscopic views of the 5 points (Pt1–Pt5) indentation are presented in Table 4 and Fig. 13 respectively.

3 Results and Discussion

The properties of hydraulic fluid (brake oil) have been described by Ajibola et al., [8,17,18] The chemical compositions and the XRD analysis of aluminium alloy specimen are presented in Tables 1 and 2 respectively. The results of the X-ray diffraction studies and microstructural examinations on the A6061 alloy showing the phases and microstructures are illustrated in the diffractogram and the micrographs in Figs. 3 and 4 respectively.
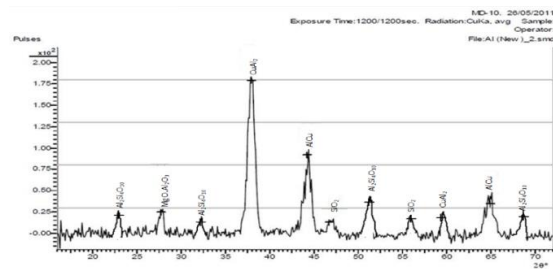
Fig. 3: The XRD diffractogram of A6061 sample

The XRD analyses shows that the bulk material consists of diverese phase microstructures being prevalent in triclinic Al$_2$Si$_4$O$_{10}$ combined with other tetragonal and monoclinic structured AlCu/CuAl and MgO.Al$_2$O$_3$ relevant to the enhanced wear resistant behaviour of the samples. The micrograph in Fig. 4 shows the grains of the wrought A6061 alloy specimen.
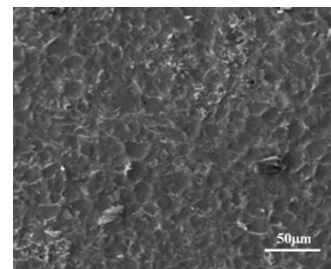
Fig. 4: Micrographs of the A6061 alloy specimens showing the as-received grains microstructure

3.1 Wear characteristics of A6061 alloy samples

The micro-photographic images that are shown in Fig. 5 (a) and (b) provide the pattern (wear topography) of groves left on the surface of the specimen by the wear jig. This gives a little useful information about the mode of wear (mechanism, topography) of the specimen in the test jig. The appearance (wear topography) are characterised with scratches on the surface of the specimens as it was observed in the case of dry test (Fig. 5a). The effect of wear due to friction is pronounced. The dry wear test (a) left deeper cut

on the surface than in the wet tests (b) after 220 mins (or 269500 wear cycles). On the other hand, Fig. 5b shows micrograph of the surface of the Al alloy after the wet wear test performed in hydraulic fluid. It points to the fact that surface topography is dependent on the properties of fluid media involved in the wear course of action.
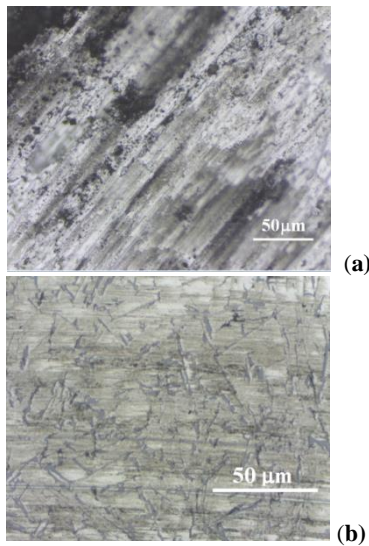

(a)

(b)

Fig. 5: Micrographs showing surfaces of specimen after (a) dry and (b) wear in the wear jig

In the plots of the wear rates (Fig. 6) and wear resistance (Fig. 7), the equations/expressions and their derivatives have been given in equations 1 to 6. The trends of the curves show increase in the wear rates with increase in time till 140 minutes (171500 cycles) for the material, after which there was reduction in the wear rates. In practice, the Al alloy specimen at that time would have been due for replacement [8]. As expected, the wrought A6061 alloy displayed significant higher wear rate under dry test condition than the specimen subjected to wet test. This is the usually behaviour of Al alloy under dry sliding as it is applicable to the dry grinding mill.
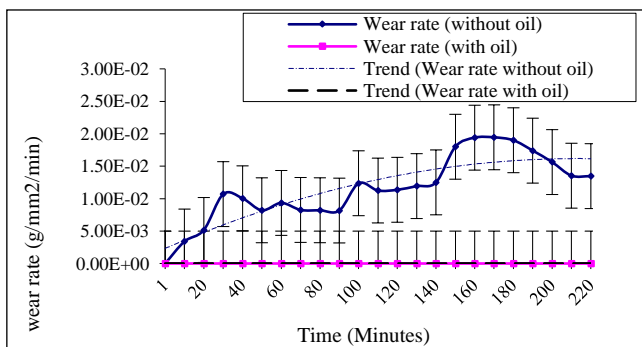

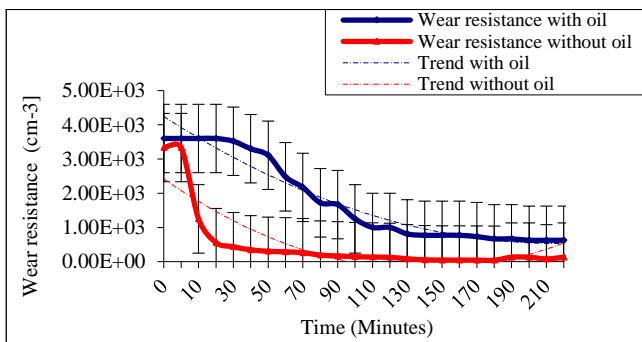Fig. 6: Wear rates of the A6061 alloy with and without oil.

Fig. 7: Wear resistance of the A6061 alloy with and without oil.

From the results, the highest wear rate of 1.40E-03 g/mm^2/min (approx.) was obtained in the wear jig run with oil. Referring to some strategic points on the wear rate curves for the discussion, Fig. 6 shows that there were cases of the regions of (i.) no wear, (ii.) constant wear, (iii.) increase in wear, and (iv.) reduction in wear. At the initial stage of the wear tests, there were active periods when no wear was experienced on the specimen. This initial stage measures the period when the material is functionally perfect under use in a system such as in the automobile master brake cylinder. This runs for a short period of 1 minute for the under dry test condition. Within the 220 (mins) time frame, the specimen has significantly higher range of wear rates of about 8.00 E-04 to 1.2 E-03 (g/mm^2/min) maximum. The mathematical trend equation is derived for the Wear rate W_r in (7),

$$W_r = -6E - 09t^2 + 2E - 07t - 1E - 07 \qquad (7)$$

where $0 \leq t \leq 220$, t = wear time (mins), W_r is the wear rate of the A6061 alloy with respect to wear time in the wear jig with fluid.

The wear resistance of the A6061 alloy surface in the wear jig (Fig. 7) shows that specimen has higher resistance in oil as compared with the dry sliding. The initial stage of the wear tests was dominated by active periods when no wear were experienced. Under the field service condition, this will correspond to a period when the material is functionally perfect (when used as piston in the automobile brake master). Within the 220 mins wear time frame, the A6061 alloy has significantly lower wear resistance range of about 625 to 3600 (cm^{-3}) in oil as compared with the dry test.

Close observation shows that within the first early wear time of 40 minutes, the surface showed constant and high wear resistance values of between 3.6E+03 to 5.0E+03 mg wear loss per cm^3 of the A6061 alloy test material. The present results show wear resistance is relatively higher as compared with what has been obtained in other previously reported experiments [8]. And for comparison of wear performance of materials under the same wear conditions, the mathematical model equations are derived for the wear resistance R_w in (8),

$$R_w = 7.2193t^2 - 341.89t + 4577.8 \qquad (8)$$

where $0 \leq t \leq 220$, t = wear time (mins), R_w is the wear resistance of the Al alloy with respect to wear time in master cylinder with brake oil. In Fig. 7, it would appear that the material is more wear resistant in the beginning of wear than on the longer running time. However, the fact is that wear rate decreases with sliding, more so when the wear volume of the specimen reduces as a result of decreasing surface contact between the specimen and the wear test jig wall.

The wear rates and wear resistance curves of Al alloy samples with the errors bars are illustrated in Fig. 6 and 7 respectively. All the plots are measured from 92 points of wear time (mins) values. Each of the point is obtained from the average value of the multiple wear tests performed on test specimens. The error bars for each of the plot give the lower and upper limit wear damages obtained from each of wear time values. For the samples, the 92 points are within the 5% the error bars for the wear rates and wear resistance of the wear time points.

3.2 Corrosion rates of samples immersed in oil.

The images in the Figs. 8a, 8b and 8c show the surface outlook of samples before and after 70 days immersion in DOT 3 at room temperature.
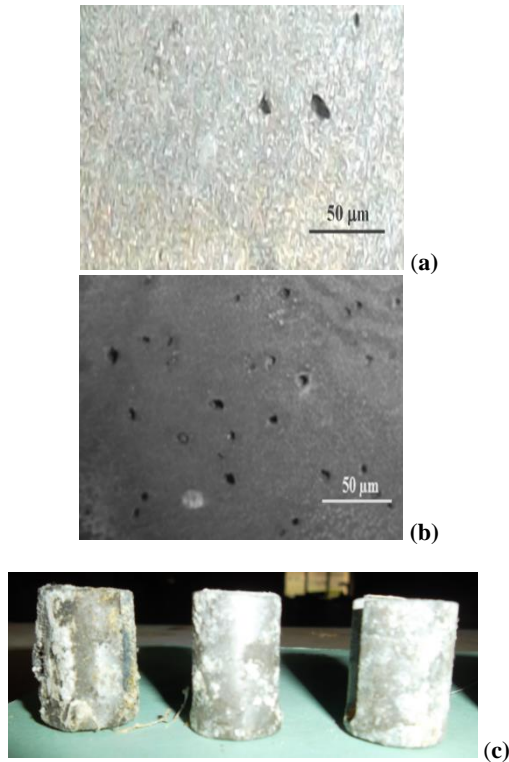
Fig. 8: Micrographs of specimen (a) before and (b) after corrosion test, (c) piston surfaces after 10 weeks immersion in brake fluid.

It was characterized with stains, discolouration and evenly distributed localised attacks in form of pits (not visible to naked eyes); thus conforming to the SAE J1703 standard. Thus it can be concluded that pitting corrosion is the prevailing corrosion mechanism. The corrosive wear is uniformly distributed over the surface. The white areas are more affected by corrosion. It was observed that the corrosive wear on the surface become significant after 4 weeks shown as layer of corrosion products was deposited in pits and on the aluminium alloy surface. The surface, as examined under microscopic camera revealed some tiny pores resulting from the corrosion of the aluminium alloy for this period of time.
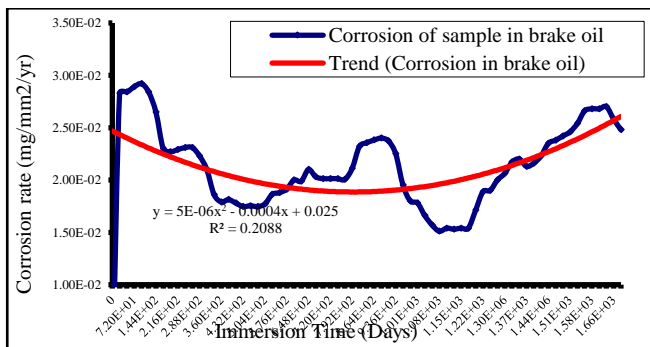

Fig. 9: Corrosion rates of wrought A6061 alloy in brake oil

Fig. 9 illustrates the polynomial curve of the second power for the trends of corrosion rates ($mg/mm^2/yr$) of Al alloy substrates in brake oil. The corrosion pattern shows trends of (i) very high corrosion rate at the initial stage of 1 week of immersion, (ii) decreasing rates at 1-2 weeks, (iii) slowly increasing at 2-4 weeks and (iv) constant corrosion rate from 4th-5th week was probably (passivation occurring) due to film formation; (v) a sudden rise in the corrosion rate at 4th-5th week (34-36th day) might be due to film break accompanied with (vi) corresponding high but constant corrosion rate and between 5th - 6th week (36 - 40 days) shows a likely another period of passivity as explained by Tabatabai et al [25]. At the initial stage, within 2 weeks (2-14 days), Al alloy corrodes at higher rates and there was gradual drop in corrosion

rate after 2 weeks (16th day). It was observed that the corrosion rate slowly reduced at 6th - 7th week (40-50 days) after which the materials experienced a period of increasing corrosion rate between 7 - 10 weeks (50 to 70 days). The Al alloy has its highest range of corrosion rate (0.020-0.030) $mg/mm^2/yr$ at the early 4 weeks (28 days) of immersion. The Al alloy corrosion rate decreases with the increasing time at 1-4 weeks (2-28 days). Objectively, the corrosion rate tests were performed to assess the level of surface degradation of the substrate in brake oil. The best fit models were developed for the trend using MS excel application of linear equations relating the amount of electroless-nickel deposited to plating bath temperature (^{o}C). The mathematical trend equation derived for the corrosion rate is (9):

$$R_c = 5E - 06t^2 - 0.0004t + 0.025 \qquad (9)$$

where $0 \le t \le 70$, t is the immersion time, R_c, is the corrosion rates of the Al alloy with respect to immersion time in brake oil. This is practically not so high when measured against the corrosion of alloys in other media [15, 26, 27]. Hence the EN coating of the as-received Al alloy surface may not be as highly necessary as it was recommended by [21] for the as-cast substrate immersed in brake oil.

3.3 Micro-structural examination Al alloy

The microstructure of the Al alloy was studied using VEGA3 TESCAN model scanning electron microscope (Fig. 10).
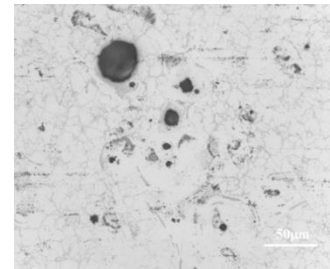

Fig. 10: Microstructure of polished wrought Al alloy specimen surface

The main features observed were pores and cracks. It is known that high amount of these defects reduce the mechanical strength of the Al material. Hence, the material has lower wear resistance as compared with the cast Al specimen worked under similar condition as presented in previous reports [16-20]. The paths of slide of the specimen against the wall of the wear jig cylinder are also marked as dotted lines across the surface of the specimen.

Figs. 11 and 12 with Table 3 illustrate the SEM images, EDX spectra lines and EDX processing data showing the compositions of the targeted areas. They show the impact of brake oil on the corrosion of the aluminium alloy specimen after 10 weeks. The EDX data show that some part of the substrate (Table 1) is found in the corrosion debris (Table 3).

Table 3: EDX data of corrosion affected area on Al-alloy substrate

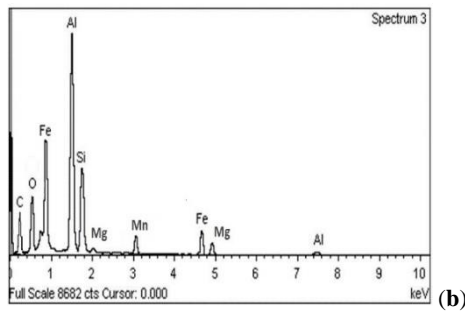| Element	Chemical composition [Wt %]						
	Mn	Fe	C	O	Al	Si	Mg
Corroded substrate	0.71	0.93	28.11	45.08	15.1	8.01	2.06
Corrosion product	-	0.33	39.24	58.10	1.66	0,67	-
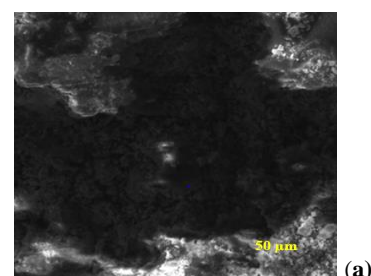
(a)

Fig. 11: Showing (a) SEM and (b) EDX spectra of corrosion affected Al-alloy substrate
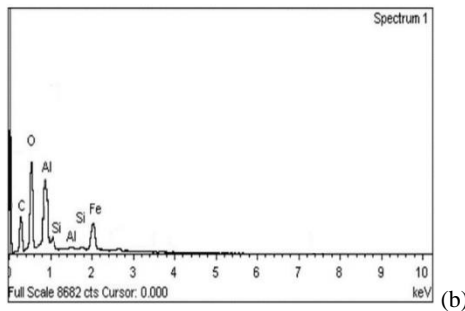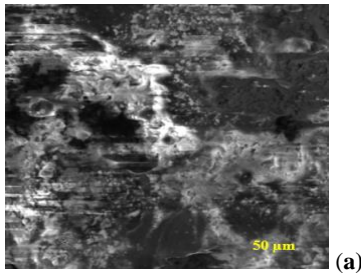

Fig. 12: Showing (a) SEM image and (b) EDX spectra of corrosion product.

From Figs 11 and 12, the SEM/EDX analyses of the corrosion product film layer performed after 70 days of immersion in the corrosive oil contained some of the elements (Al, Fe and Si) in the formed film. The layer of corrosion product obtained from the aluminium alloy-oil reaction (with the brake oil environment) showed the formation is associated with the pit surroundings whereby the oxides are formed in amorphous phase. Contrary to the SAE J1703 specification, the formed deposits seemly appeared jelly-like but not crystalline as illustrated in Fig. 8c. This suggests that moisture was likely absorbed into the fluid system within the 10 weeks of experimentation.

3.4 Hardness test of samples

The results of micro-hardness test of samples are presented in Table 4. The results shows that the specimen has lower range of hardness, thus the wear rate which is a function of the hardness of material should also be comparatively lower to the sand cast specimen reported [8, 16].

Table 4: Micro-hardness test of sample

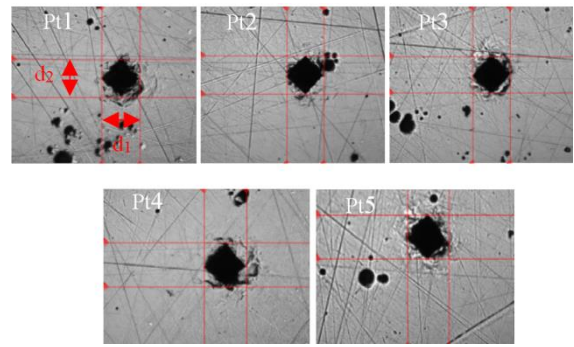|	Vicker's No (HV/0.5)				
Samples	Pt 1	Pt 2	Pt 3	Pt 4	Pt5
Al 1	53.9	54.4	57.3	51.3	54.8
Analysis	Max 57.26; Min 51.27; Average 54.31; Std.dev 1.92				
Indentation d_1(mm)	0.1315	0.1282	0.1290	0.1315	0.1352
Indentation d_2(mm)	0.1309	0.1329	0.1255	0.1375	0.1250

Fig. 13: Micrographs showing the points of indentations

3.5 Wear and corrosion of Al-alloy substrate in oil.

For the specimen that is subjected to a condition under tribocorrosion, the synergistic constituent $S_{(C,W)}$ forms part of the overall damage that results from the combination of material corrosion in fluid and the wear processes. The total loss, $T_{(C,W)}$, is interrelated with the synergism by Equations (10).

$$T_{(C,W)} = W_o + C_o + S_{(C,W)} \tag{10}$$

where $T_{(C,W)}$ is the whole material loss or damage, $S_{(C,W)}$ is the synergetic component of the overall corrosion in fluid, W_o is the mechanical wear in the absence of fluid and C_o is the measured electrochemical loss due corrosion only.

In this report, the concept of tribocorrosion and synergism cannot be applied to interpret or justify the total damage rate. This is because; the measurements of corrosion and wear were conducted under two different settings.

However, based on the hydraulic brake master cylinder/piston system, it is evident that the most prevailing factors/conditions of damage done on the materials are due to mechanical wear $W_{(o,m)}$ (in the presence of brake oil), and purely corrosion C_o, (when the brake system is at rest or the car is parked for a quite long time). Thus in the cylinder-piston-brake oil interaction, the total damage (loss) $T_{(C,W)}$ in that instance is given by; loss to mechanical wear (in the presence of brake oil) + loss to corrosion. The mechanical wear loss (in the presence of brake oil) is reported in Fig 6 while the loss to corrosion is Fig 9.

The behaviour of the Al alloy in the brake fluid subjected to wear and corrosion conducted under different set-up could be interpreted as in the Equations 11-14. The entire components damage occurring from the Al alloys wear and corrosion processes in brake fluid are obtained from Fig. 6 and 9.

Under a wet wear condition, the total material damage rate, $T_{(C,W)}$ relates to wear and corrosion by the Equations 11-14.

$$T_{(C,W)} = C_o + W_{(o,m)} \tag{11}$$

For a wet wear condition,

$$W_{(o,m)} = 6.85E - 13t^2 + 2.28E - 11t - 1.14E - 11 \tag{12}$$

For condition under corrosion only

$$C_o = 1.37E - 09t^2 + 1.10E - 06t + 6.85E - 05 \tag{13}$$

where t is the exposure time (yr), $T_{(C,W)}$ is the total material damage due to corrosion and mechanical wear, $W_{(om)}$ is the mechanical wear damages measured in oil, C_o is the corrosion damage for the Al alloy in oil.

Using (11), equations (12) and (13) are combined to get the total material loss rate $(T_{(C,W)})$ in g/mm²/yr for Al alloy in (14).

$$T_{(C,W)} = 1.37E - 09t^2 + 1.10E - 06t + 6.85E - 05 \tag{14}$$

where t is the exposure time (yr), $T_{(C,W)}$ is the total material damage rate due to corrosion and mechanical wear.

In the case of a non-lubricating dry condition, the total material loss, $T_{(C,W)}$ in (11) is related to mechanical wear only as expressed in (15);

$$T_{(C,W)} = W_o \qquad (15)$$
$$W_o = 3.43E - 09\ t^2 + 1.37E - 07t + 1.94E - 07 \qquad (16)$$

where t is the exposure time (yr), W_o is the wear damage of the Al alloy in the absence of oil or corrosion.

The current study involves the dynamic variation of wear characteristics, the interaction between two contacting Al alloy specimens (master cylinder and piston) immersed in brake oil. The collective effects of wear, W, and corrosion, C, that often result in total damage rates will be much greater than the additive effects of wear or corrosion taken alone according to ASTM G-119-04 [24].

The microstructures and results of surface corrosion examinations presented in Fig. 8-12 and Table 3 offer some little useful information about (i) the nature of the Al alloy material and (ii) corrosion damage mechanisms. Fig. 8 shows that pitting seems to have occurred and oxide is formed on the aluminium specimen surface (Fig. 11-12) which is well known even under common atmospheric moisturised conditions. The primary Al alloy (Fig. 10) are characterised with some large size equiaxed grains and some internal production deficiencies (pores and cracks). Grain size has for a long time been identified to affect the mechanical properties (strength, hardness) of metallic alloy component. Thus, the large size equiaxed grains observed in the Al alloy seems to influence the higher wear rate and enhanced corrosion resistance as compared with small sized grain structured cast Al alloy available in the literature reports [8,16-20].

The present study shows significant differences in the mechanical wear behaviour of the wrought Al alloy when compared with the cast Al alloy samples reported previously. Particularly, the specimen demonstrated lower wear resistance and higher corrosion rate than the cast specimen results reported in previous works [18,19]. The reasons for such obtained results have been also explained in the metallurgy of the cast Al alloy specimens [19]. The present results fall within reach to understanding the performance and the differences in the wear properties of the test samples previously reported by Ajibola et al., [20]. The corrosion rate is comparatively lower than what is obtained for other Al alloy types and steels in other media (such as acid and alkali) as reported in the literatures [5, 15, 17, 27].

4   Conclusions

The extent of wear and corrosion of the 6061 aluminium alloy specimen in brake fluid have been studied and the following summaries are drawn from the results obtained. In case of the use of the 6061 aluminium alloy specimen as the master brake piston component in the presence of brake fluid, the dry wear testing has little value for practical applications. The A6061 alloy materials in wet wear test has the highest value of 5.24E-07 mg/mm^2/cycle (after 130 minutes) and corrosion rate of 0.0292 mg/mm^2/yr after the first 7 days (168 hrs) of immersion in brake fluid. This is reasonably not so high when compared with the previously reported corrosion rate results of cast Al alloy in brake fluid media. The implication is that; since the material has much lower wear rate but high corrosion rate at the early stage of its immersion in the fluid, a less corrosive environment could be imposed by using inhibitor. This will reduce the total material loss of the material when used under wet condition.

Acknowledgement

Conflict of Interests

The authors declare that there is no conflict of interests as regarding the publication of this paper.

References

[1]   ASM International, "Friction, Lubrication, and Wear Technology", *The ASM Handbook* Vol. 18 (1992), pp1,

[2]   Bronček J., Dzimko M., Hadzima B, Takeichi Y. "Experimental investigations of aluminium alloys 2024 –T 3 form in terms of tribocorrosion characteristics". *Acta Metallurgica Slovaca,* Vol. 20, No. 1, (2014), pp. 97-104, DOI 10.12776/ams.v20i1.273 p-

[3]   Ponthiaux P, Wenger F and Celis J. "Tribocorrosion: Material behavior under combined conditions of corrosion and mechanical loading, Corrosion Resistance", Dr Shih (Ed.), (2012). InTech, Available from: http://www.intechopen.com/books/corrosion-resistance/tribocorrosionmaterial-behaviour-under-combined-conditions-of-corrosion-and-mechanical-loading

[4]   Ajibola O.O, Oloruntoba D. T., Adewuyi B.O. "Effect of processing parameters on the protective quality of Electroless-Ni on cast aluminium alloy", *Journal of Metallurgy,* Volume 2015, Article ID 386347, 12 pages. http://dx.doi.org/10.1155/2015/386347

[5]   Ajibola O.O, Adebayo A.O., Oloruntoba D. T. "Corrosion of heat treated Electroless-Ni plated mild carbon steels in dilute H$_2$SO$_4$". *International Journal of Materials Science and Applications. Vol.*4 No 5, (2015), pp333-342. doi: 10.11648/j.ijmsa.20150405.18.

[6]   Ajibola O.O, Oloruntoba D. T., Adewuyi B.O. "Effect of hard surface grinding and activation on electroless-nickel plating on cast aluminium alloy substrates". *Journal of Coatings.* Volume 2014, Article ID 841619, 10 pages. http://dx.doi.org/10.1155/2014/841619

[7]   Ajibola O.O, Oloruntoba D. T., Adewuyi B.O. "Effect of polishing grits, temperatures and selected activators on electroless-nickel deposition on cast aluminium substrates". *Journal – The Institution of Engineers, Malaysia,* Vol. 76, No. 1, (2015), pp38-46.

[8]   Ajibola O.O., Adewuyi B.O., and Oloruntoba D.T. "Wear behaviour of sand cast eutectic Al-Si alloy in hydraulic brake fluid", *International Journal of Innovation and Applied Studies,* Vol.6, No 3, (2014), pp420-430.

[9]   Rendahl B.O and LeBozec N.. "Corrosion resistance of automotive materials: from laboratory to field exposures". *Eurocorr 2011, Stockholm, Sweden,* No 1033. (2011)

[10] Pokhmurskii V., Zin I, Vynar V., Pokhmurska H., Lampke T., "Conventional electrochemical and micro-electrochemical techniques for studies of tribocorrosion on 2024 aluminium alloy". *Eurocorr 2011, Stockholm, Sweden*, No 4914. (2011)

[11] Geringer J., Normand B., Alemany-Dumont C., Diemiaszonek R. "Copper and aluminium tribocorrosion in acid medium: Electrochemical Impedance Spectroscopy investigations". *Eurocorr 2009, Nice, France.* (2009), p.14.

[12] https://en.wikipedia.org/wiki/Brake_fluid. Accessed on 01-April-2017

[13] http://www.wiki/sae/ accessed on 16-04-2012

[14] Robert Bosch GmbH. 2007. *Bosch Automotive Handbook.* 7th ed. Bentley Publishers, Robert Bentley iNC, (2007).

[15] Ademoh N.A "Inhibition characteristics of watermelon oil on aluminium in acid and saline water". *Assumption University Journal of Technology.* Vol.15, No 4, (2012), pp265-272. http://www.journal.au.edu/au_techno/2012/apr2012/journal154_article09.pdf

[16] Ajibola O.O, Oloruntoba D. T., Adewuyi B.O. "Metallurgical study of cast aluminium alloy used in hydraulic master brake

calliper", *International Journal of Innovation and Scientific Research*. Vol.8, No 2, (2014), pp324-333.

[17] Ajibola O.O, Oloruntoba D.T. "Wear and corrosion of cast Al alloy piston with and without brake oil". *Indian Journal of Materials Science*, Volume 2015, Article ID 763618, (2015), 10 pages

[18] Ajibola O.O, Oloruntoba D. T., Adewuyi B.O. "Design and performance evaluation of wear test jig for aluminium alloy substrate in hydraulic fluid". *African Corrosion Journal,* Vol 1, No, 1, (2015), pp 40-45. DOI: 10.13140/2.1.4363.5844

[19] Ajibola O.O, Oloruntoba D. T., "Effect of MgFeSi inoculants on properties of Cast 6061 Al Alloy for brake master piston application", *Indian Journal of Materials Science*, Volume 2015, Article ID 756219, 10 pages. http://dx.doi.org/10.1155/2015/756219

[20] Ajibola O.O, Oloruntoba D. T., Adewuyi B.O. "Effects of moulding sand permeability and pouring temperatures on properties of cast 6061 Aluminium alloy". *International Journal of Metals,* Volume 2015, Article ID 632021, 13 pages, 2015.

[21] Ajibola O.O, Oloruntoba D. T., Adewuyi B.O. "Investigation of corrosion of cast aluminium alloy piston in brake fluid". *African Corrosion Journal*, Vol 2, No, 2, (2016) pp 1-11.

[22] Pari H, Raj R, Pandiarajan G, Rasu E., "Study on the performance of electroless nickel coating on aluminium for cylinder liners". *Patent No. F2008-SC-015*

[23] Elansezhian R., Ramamoorthy B., Kesavan N.P., "Effect of surfactants on the mechanical properties of electroless (Ni–P) coating". *Surface and Coatings Technology*, Vol.203, No (5–7), (2008), pp 709–712.

[24] ASTM Designation G 119 – 03: "Standard guide for determining synergism between wear and corrosion". ASTM Designation G 119, (2003), pp1-6

[25] Tabatabai D., Szillies S., Feil F., Grundmeier G., Fürbeth W. "Self-healing corrosion protective coatings for magnesium alloys by modifying anodizing layers with corrosion inhibitors". *Eurocorr 2011, Stockholm, Sweden*, No 4575. (2011).

[26] Adewuyi B.O. "The influence of Fe variation on the corrosion behaviour of heat treated aluminium alloys in tomato juice". *Nigerian Journal of Technology*, Vol. 21, No. 1, (2002), pp72-78.

[27] Alaneme K.K., Adewale T.M., Olubambi P.A. "Corrosion and wear behaviour of Al–Mg–Si alloy matrix hybrid composites reinforced with rice husk ash and silicon carbide". *Journal of Materials Research and Technology,* Vol.3, No 1, (2013), pp9-16.